Topological Reorganization of Gallium–Sulfido Clusters

Michael B. Power,[1a] Joseph W. Ziller,[1b] and Andrew R. Barron*,[1a]

Departments of Chemistry, Harvard University, Cambridge, Massachusetts 02138, and University of California, Irvine, California 92717

Received March 24, 1992

The prolonged thermolysis of $[(^tBu)GaS]_4$ in hexane results in the formation of the heptamer $[(^tBu)GaS]_7$ (1), while in pentane the octamer $[(^tBu)GaS]_8$ is formed in low yield. Dissolution of $[(^tBu)GaS]_x$ (x = 4, 7, 8) in pyridine yields the trimeric pyridine complex $[(^tBu)Ga(S)py]_3$ (2). Sublimation of 2 regenerates the tetramer, while thermolysis in the solid state yields the hexamer $[(^tBu)GaS]_6$ (3), which is reconverted to 2 on addition of pyridine. While compound 1 sublimes intact under vacuum, at atmospheric pressure compounds 1 and 3 sublime to yield the tetramer. The synthesis of the first gallium oxide cage compound, the nonameric $[(^tBu)GaO]_9$ (4), is reported. The molecular structures of 1–3 have been determined by X-ray crystallography. The relationship between $[(^tBu)GaS]_x$, the analogous iron–sulfide clusters $[(L)FeS]_x$, and the iminoalanes $[RAl(NR')]_x$ is discussed. Crystal data for 1: monoclinic, $P2_1/n$, a = 10.491 (2) Å, b = 21.697 (5) Å, c = 41.383 (7) Å, β = 95.34 (2)°, Z = 8, R = 0.059, R_w = 0.071. Crystal data for 2: monoclinic, $P2_1/c$, a = 9.377 (5) Å, b = 15.832 (4) Å, c = 22.471 (7) Å, β = 98.42 (3)°, Z = 4, R = 0.047, R_w = 0.059. Crystal data for 3: orthorhombic, *Cmca*, a = 20.67 (1) Å, b = 9.116 (5) Å, c = 20.90 (1) Å, Z = 4, R = 0.058, R_w = 0.072.

Introduction

We have recently reported the synthesis and structural characterization of the cubane clusters $[(^tBu)GaE]_4$ (E = S, Se, Te) (I, E = S).[2,3] In the case of the sulfide $[(^tBu)GaS]_4$, we observed that repeated sublimation results in the formation of the octamer $[(^tBu)GaS]_8$, in low yield. Although we were unable to isolate the octamer pure, mass spectral and NMR data were consistent with a drum structure (II) similar to those observed for tin oxide clusters.[4] Despite the low yield of tetramer to octamer

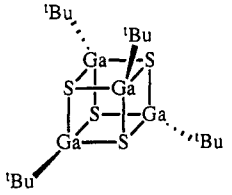

I

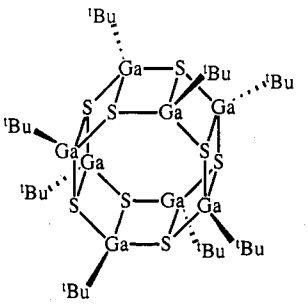

II

conversion, this intriguing observation suggested that facile cluster rearrangements may occur to give higher nuclearity clusters. We have, therefore, investigated the thermal and Lewis base assisted topological rearrangement of the gallium–sulfido cubane. The results of this study are presented herein, along with the synthesis and characterization of the first gallium–oxo cluster, $[(^tBu)GaO]_9$.

Results and Discussion

Gallium–Sulfido Clusters. The reactions studied are summarized in Scheme I. Prolonged thermolysis of $[^tBuGaS]_4$ in refluxing hexane results in its near-quantitative conversion to a single new species, the mass spectrum of which exhibits a peak due to the parent ion of the heptamer $[(^tBu)GaS]_7$ (1), while the ^1H and ^{13}C NMR spectra are consistent with three gallium-coordinated *tert*-butyl environments (1:3:3) (see Experimental Section). Like $[(^tBu)GaS]_4$, the heptamer 1 is stable to oxidation and hydrolysis, both as a solid and in solution. Compound 1 sublimes intact under vacuum (240 °C, 10^{-3} Torr); however, it yields only $[(^tBu)GaS]_4$ when sublimed at atmospheric pressure. Compound 1 may also be formed in excellent yield (>80%) by the solid-state thermolysis of $[(^tBu)GaS]_4$ in a sealed tube at 175 °C (see Experimental Section).

Scheme I[a]

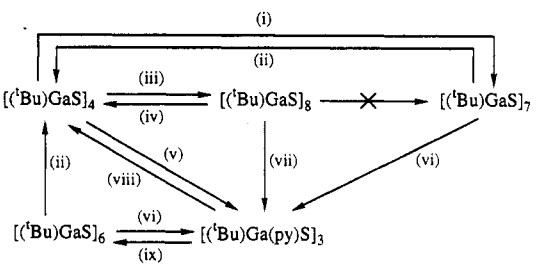

[a] Legend: (i) Δ, hexane, 3–4 days; (ii) sublimation, 1 atm; (iii) Δ, pentane, 12 h; (iv) Δ, pentane; (v) pyridine, minutes; (vi) pyridine, 1–2 days; (vii) Δ, pyridine; (viii) vacuum sublimation; (ix) Δ, solid state.

The molecular structure of $[(^tBu)GaS]_7$, as determined by X-ray crystallography, is shown in Figure 1; selected bond lengths and angles are given in Table I. Two crystallographically independent but chemically equivalent molecules are present within the asymmetric unit. The cluster consists of a cage structure of seven gallium atoms and seven μ_3-sulfido groups. The pseudotetrahedral coordination sphere at each gallium is completed by a terminally bound *tert*-butyl group. The Ga_7S_7 core may conceptually be considered to be derived from the linkage of two apically-deficient cubanes, i.e., $(^tBu)_4Ga_4S_3$ and $(^tBu)_3Ga_3S_4$, and is similar to those reported for $[RAl(NMe)]_7$ (R = Me, Et)[5] and that proposed for $[EtMgO^nPr]_7$.[6] The solid-state structure is entirely consistent with NMR spectroscopy (see Experimental Section), indicating that the cage structure is retained in solution. The Ga–S bond lengths in $[(^tBu)GaS]_7$ fall into two groups; those linking, and those of, the apically-deficient cubane

* To whom all correspondence should be addressed.

(1) (a) Harvard University. (b) University of California, Irvine.
(2) Power, M. B.; Barron, A. R. *J. Chem. Soc., Chem. Commun* **1991**, 1315.
(3) Power, M. B.; Ziller, J. W.; Tyler, A. N.; Barron, A. R. *Organometallics* **1992**, *11*, 1055.
(4) See for example: Holmes, R. R. *Acc. Chem. Res.* **1989**, *22*, 190.
(5) (a) Hitchcock, P. B.; Smith, J. D.; Thomas, K. M. *J. Chem. Soc., Dalton Trans.* **1976**, 1433. (b) Gosling, K.; Smith, J. D.; Wharmby, D. H. W. *J. Chem. Soc. A* **1969**, 1738.
(6) Coates, G. E.; Heslop, J. A.; Redwood, M. E.; Ridley, D. *J. Chem. Soc. A* **1968**, 1118.

0276-7333/92/2311-2783$03.00/0

Table I. Selected Bond Lengths (Å) and Angles (deg) in [(ᵗBu)GaS]₇ (1)

molecule 1		molecule 2		molecule 1		molecule 2	
Ga(1)–S(1)	2.372 (2)	Ga(8)–S(8)	2.358 (4)	Ga(4)–S(4)	2.303 (4)	Ga(11)S(11)	2.295 (4)
Ga(1)–S(2)	2.361 (4)	Ga(8)–S(9)	2.361 (4)	Ga(4)–C(1)	1.97 (1)	Ga(11)–C(41)	1.96 (1)
Ga(1)–S(3)	2.368 (4)	Ga(8)–S(10)	2.364 (4)	Ga(S)–S(4)	2.321 (4)	Ga(12)–S(11)	2.317 (4)
Ga(1)–C(1)	1.96 (1)	Ga(8)–C(29)	1.98 (1)	Ga(5)–S(5)	2.318 (4)	Ga(12)–S(12)	2.328 (4)
Ga(2)–S(1)	2.339 (4)	Ga(9)–S(8)	2.337 (4)	Ga(5)–S(7)	2.366 (4)	Ga(12)–S(14)	2.353 (4)
Ga(2)–S(3)	2.336 (4)	Ga(9)–S(10)	2.326 (4)	Ga(5)–C(17)	1.95 (1)	Ga(12)–C(45)	1.95 (1)
Ga(2)–S(5)	2.301 (4)	Ga(9)–S(12)	2.291 (4)	Ga(6)–S(5)	2.318 (4)	Ga(13)–S(12)	2.321 (4)
Ga(2)–C(5)	1.96 (1)	Ga(9)–C(33)	1.97 (1)	Ga(6)–S(6)	2.319 (4)	Ga(13)–S(13)	2.319 (4)
Ga(3)–S(1)	2.327 (4)	Ga(10)–S(8)	2.332 (4)	Ga(6)–S(7)	2.350 (4)	Ga(13)–S(14)	2.346 (4)
Ga(3)–S(2)	2.330 (4)	Ga(10)–S(9)	2.329 (4)	Ga(6)–C(21)	1.97 (1)	Ga(13)–C(49)	1.97 (1)
Ga(3)–S(6)	2.287 (4)	Ga(10)–S(13)	2.282 (4)	Ga(7)–S(4)	2.311 (4)	Ga(14)–S(11)	2.318 (4)
Ga(3)–C(9)	2.01 (1)	Ga(10)–C(37)	2.00 (1)	Ga(7)–S(6)	2.314 (4)	Ga(14)–S(13)	2.303 (4)
Ga(4)–S(2)	2.331 (4)	Ga(11)–S(9)	2.324 (4)	Ga(7)–S(7)	2.360 (4)	Ga(14)–S(14)	2.354 (4)
Ga(4)–S(3)	2.345 (4)	Ga(11)–S(10)	2.333 (4)	Ga(7)–C(25)	21.98 (1)	Ga(14)–C(53)	1.99 (1)
S(1)–Ga(1)–S(2)	96.1 (1)	S(8)–Ga(8)–S(9)	96.7 (1)	Ga(1)–S(1)–Ga(2)	82.1 (1)	Ga(8)–S(8)–Ga(9)	82.6 (1)
S(1)–Ga(1)–S(3)	96.4 (1)	S(8)–Ga(8)–S(10)	96.0 (1)	Ga(1)–S(1)–Ga(3)	82.3 (1)	Ga(8)–S(8)–Ga(10)	82.0 (1)
S(2)–Ga(1)–S(3)	96.7 (1)	S(9)–Ga(8)–S(10)	96.4 (1)	Ga(2)–S(1)–Ga(3)	110.7 (1)	Ga(9)–S(8)–Ga(10)	111.1 (1)
S(1)–Ga(2)–S(3)	98.2 (1)	S(8)–Ga(9)–S(10)	97.6 (1)	Ga(1)–S(2)–Ga(3)	82.4 (1)	Ga(8)–S(9)–Ga(10)	82.0 (1)
S(1)–Ga(2)–S(5)	114.1 (1)	S(8)–Ga(9)–S(12)	115.1 (1)	Ga(1)–S(2)–Ga(4)	82.1 (1)	Ga(8)–S(9)–Ga(11)	82.3 (1)
S(3)–Ga(2)–S(5)	114.7 (1)	S(10)–Ga(9)–S(12)	113.3 (1)	Ga(3)–S(2)–Ga(4)	111.1 (2)	Ga(10)–S(9)–Ga(11)	82.7 (1)
S(1)–Ga(3)–S(2)	98.2 (1)	S(8)–Ga(10)–S(9)	98.3 (1)	Ga(1)–S(3)–Ga(4)	81.8 (1)	Ga(8)–S(10)–Ga(11)	82.1 (1)
S(1)–Ga(3)–S(6)	115.2 (1)	S(8)–Ga(10)–S(13)	113.9 (1)	Ga(2)–S(3)–Ga(4)	110.2 (1)	Ga(9)–S(10)–Ga(11)	111.4 (1)
S(2)–Ga(3)–S(6)	113.4 (1)	S(9)–Ga(10)–S(13)	115.5 (1)	Ga(4)–S(4)–Ga(5)	116.4 (2)	Ga(11)–S(11)–Ga(12)	115.5 (2)
S(2)–Ga(4)–S(3)	98.2 (1)	S(9)–Ga(11)–S(10)	98.3 (1)	Ga(4)–S(4)–Ga(7)	116.1 (2)	Ga(11)–S(11)–Ga(14)	118.1 (2)
S(2)–Ga(4)–S(4)	114.6 (1)	S(9)–Ga(11)–S(11)	113.4 (1)	Ga(5)–S(4)–Ga(7)	84.9 (1)	Ga(12)–S(11)–Ga(14)	85.0 (1)
S(3)–Ga(4)–S(4)	114.6 (1)	S(10)–Ga(11)–S(11)	115.3 (1)	Ga(2)–S(5)–Ga(5)	116.6 (2)	Ga(9)–S(12)–Ga(12)	117.3 (2)
S(4)–Ga(5)–S(5)	114.2 (1)	S(11)–Ga(12)–S(12)	114.4 (1)	Ga(2)–S(5)–Ga(6)	116.2 (2)	Ga(9)–S(12)–Ga(13)	115.0 (2)
S(4)–Ga(5)–S(7)	93.9 (1)	S(11)–Ga(12)–S(14)	94.0 (1)	Ga(5)–S(5)–Ga(6)	85.5 (1)	Ga(12)–S(12)–Ga(13)	84.8 (1)
S(5)–Ga(5)–S(7)	93.0 (1)	S(12)–Ga(12)–S(14)	93.1 (1)	Ga(3)–S(6)–Ga(6)	115.7 (2)	Ga(10)–S(13)–Ga(13)	116.3 (2)
S(5)–Ga(6)–S(6)	114.5 (1)	S(12)–Ga(13)–S(13)	115.3 (1)	Ga(3)–S(6)–Ga(7)	117.6 (2)	Ga(10)–S(13)–Ga(14)	116.7 (2)
S(5)–Ga(6)–S(7)	93.4 (1)	S(12)–Ga(13)–S(14)	93.5 (1)	Ga(6)–S(6)–Ga(7)	84.9 (1)	Ga(13)–S(13)–Ga(14)	85.0 (1)
S(6)–Ga(6)–S(7)	93.9 (1)	S(13)–Ga(13)–S(14)	93.8 (1)	Ga(5)–S(7)–Ga(6)	83.7 (1)	Ga(12)–S(14)–Ga(13)	83.7 (1)
S(4)–Ga(7)–S(6)	114.6 (1)	S(11)–Ga(14)–S(13)	113.6 (1)	Ga(5)–S(7)–Ga(7)	82.8 (1)	Ga(12)–S(14)–Ga(14)	83.4 (1)
S(4)–Ga(7)–S(7)	94.3 (1)	S(11)–Ga(14)–S(14)	93.9 (2)	Ga(6)–S(7)–Ga(7)	83.2 (1)	Ga(13)–S(14)–Ga(14)	83.2 (1)
S(6)–Ga(7)–S(7)	93.8 (1)	S(13)–Ga(14)–S(14)	94.0 (1)				

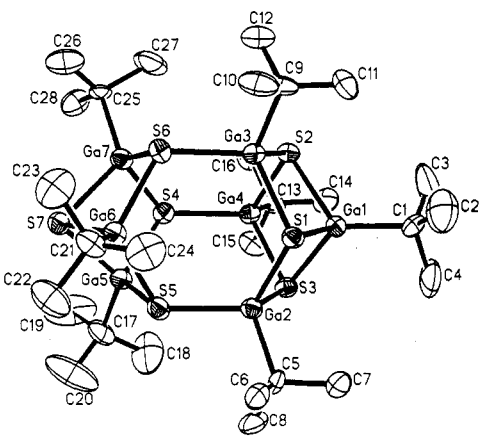

Figure 1. Molecular structure of one of the independent molecules of [(ᵗBu)GaS]₇ (1) present in the asymmetric unit. Thermal ellipsoids are shown at the 50% probability level, and hydrogen atoms are omitted for clarity.

fragments (Ga–S_{av} = 2.292 (4) and 2.334 (5) Å, respectively). The latter are comparable to that observed for the cubane [(ᵗBu)GaS]₄ (2.359 (3) Å),[2,3] while the former is within the range observed in the adamantane-like $Ga_4I_4(SMe)_4S_2$ (2.204 (8) Å)[7] and $[Ga_4S_{10}]^{8-}$ (2.289 (2) Å).[8] These differences are consistent with the strain inherent in the cubane-derived structure.

The formation of [(ᵗBu)GaS]₇ from [(ᵗBu)GaS]₄ may suggest that the latter dimerizes to give an octamer, which subsequently decomposes to the heptamer. However, although an octamer, [(ᵗBu)GaS]₈, is formed in low yield from [(ᵗBu)GaS]₄, upon the thermolysis in pentane of the latter, and may be isolated by washing with pyridine (see below), there is no evidence to indicate that the octamer is converted to the heptamer under more forcing conditions. Instead, we believe that [(ᵗBu)GaS]₈ initially reforms the tetramer, which over time is subsequently converted to the heptamer (see Scheme I). The tetramer is also formed as the major product from the vacuum sublimation of the octamer.

The isolation of a sample of the octamer devoid of tetramer has allowed us to obtain the ^{13}C NMR and IR spectral data (see Experimental Section) to augment the ^1H NMR and mass spectral characterization previously reported. We have, however, been unable to obtain crystals suitable for X-ray crystallography to confirm our previously proposed structure (II). The presence of a single resonance for the *tert*-butyl groups in both ^1H and ^{13}C does, in the absence of an unlikely pathological overlap of all resonances, proclude a structure analogous to that reported for [HAl(Nⁿ Pr)]₈[9] and [MeAl(NMe)]₈,[10] i.e., III, for which two distinct sets of resonances should be observed.

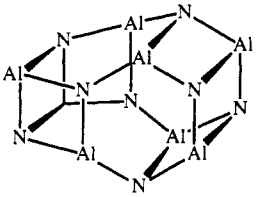

III

(7) Boardman, A.; Jeffs, S. E.; Small, R. W. H.; Worrall, I. J. *Inorg. Chim. Acta* **1984**, *83*, L39.
(8) Krebs, B.; Voelker, D.; Stiller, K. *Inorg. Chim. Acta* **1982**, *65*, L101.
(9) DelPiero, G.; Cesari. M.; Perego, G.; Cucinella, S.; Cernia, E. *J. Organomet. Chem.* **1977**, *129*, 289.
(10) Amirkhalili, S.; Hitchcock, P. B.; Smith, J. D. *J. Chem. Soc., Dalton Trans.* **1979**, 1206.

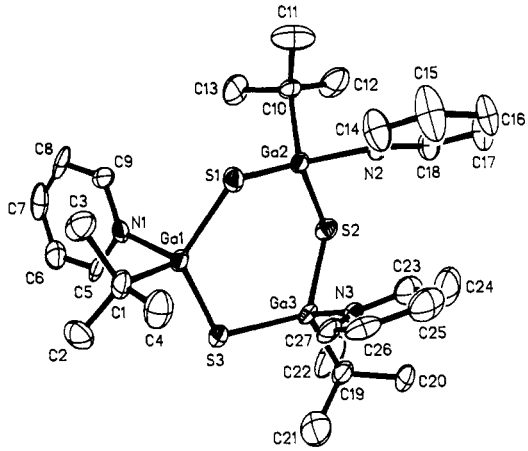

Figure 2. Molecular structure of $[(^tBu)Ga(S)py]_3$ (**2**). Thermal ellipsoids are shown at the 40% probability level, and hydrogen atoms are omitted for clarity.

Table II. Selected Bond Lengths (Å) and Angles (deg) for $[(^tBu)Ga(S)py]_3$ (2)

Ga(1)–S(1)	2.235 (3)	Ga(1)–S(3)	2.247 (3)
Ga(1)–C(1)	2.003 (10)	Ga(1)–N(1)	2.100 (8)
Ga(2)–S(1)	2.253 (3)	Ga(2)–S(2)	2.231 (3)
Ga(2)–C(10)	2.001 (9)	Ga(2)–N(2)	2.122 (8)
Ga(3)–S(2)	2.249 (3)	Ga(3)–S(3)	2.237 (3)
Ga(3)–C(19)	2.002 (10)	Ga(3)–N(3)	2.078 (8)
S(1)–Ga(1)–S(3)	122.4 (1)	S(1)–Ga(1)–C(1)	110.8 (3)
S(3)–Ga(1)–C(1)	113.5 (3)	S(1)–Ga(1)–N(1)	105.5 (2)
S(3)–Ga(1)–N(1)	101.2 (2)	C(1)–Ga(1)–N(1)	99.8 (3)
S(1)–Ga(2)–S(2)	121.5 (1)	S(1)–Ga(2)–C(10)	114.3 (3)
S(2)–Ga(2)–C(10)	112.8 (3)	S(1)–Ga(2)–N(2)	100.4 (2)
S(2)–Ga(2)–N(2)	102.3 (2)	C(10)–Ga(2)–N(2)	101.3 (3)
S(2)–Ga(3)–S(3)	119.8 (1)	S(2)–Ga(3)–C(19)	111.5 (3)
S(3)–Ga(3)–C(19)	112.5 (3)	S(2)–Ga(3)–N(3)	101.7 (3)
S(3)–Ga(3)–N(3)	102.4 (2)	C(19)–Ga(3)–N(3)	107.0 (4)
Ga(1)–S(1)–Ga(2)	112.6 (1)	Ga(2)–S(2)–Ga(3)	107.3 (1)
Ga(1)–S(3)–Ga(3)	107.9 (1)		

Dissolution of $[(^tBu)GaS]_n$ (n = 4, 7, 8) in pyridine results in the formation of a compound formulated, from ^1H and ^{13}C NMR spectroscopy, as $(^tBu)Ga(S)py$ (**2**) (see Scheme I and Experimental Section). Since the molecularity could not be determined from mass spectrometry (see below), an X-ray crystallographic determination was undertaken, which shows it to be trimeric in the solid state, i.e., $[(^tBu)Ga(S)py]_3$.

The molecular structure of $[(^tBu)Ga(S)py]_3$ is shown in Figure 2; selected bond lengths and angles are given in Table II. The six-membered Ga_3S_3 cycle has, as can be seen from Figure 3, a twist-boat conformation,[11] with the pyridine ligands occupying the pseudoaxial sites. The μ_2-sulfido bridges are close to symmetrical, and the Ga–S distances (2.231 (3)–2.253 (3) Å) are within the range observed for the μ_3-sulfido bridges, linking the halves of the heptamer (see above). The Ga–C ($Ga–C_{av}$ = 2.00 (1) Å) and Ga–N ($Ga–N_{av}$ = 2.100 (8) Å) distances are close to their expected values.[12,13]

The rate of dissolution/reaction of the sulfido clusters with pyridine is dependent on the cluster size; the tetramer dissolves rapidly in minutes, and the hexamer (below) and the heptamer dissolve over a period of hours, while the octamer requires gentle warming. Thus, the octamer is readily separated from the tetramer by washing with pyridine (see Experimental Section).

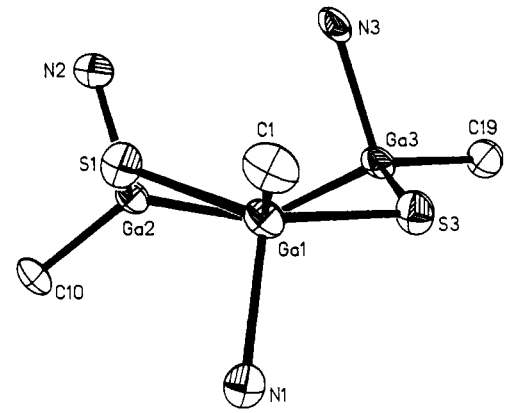

Figure 3. The Ga_3S_3 core of $[(^tBu)Ga(S)py]_3$ (**2**) viewed along the Ga(1)···S(2) vector. Thermal ellipsoids are shown at the 40% probability level. Pyridine carbon and *tert*-butyl methyl groups are omitted for clarity.

Table III. Selected Bond Lengths (Å) and Angles (deg) for $[(^tBu)GaS]_6$ (3)

Ga(1)–S(1)	2.323 (3)	Ga(1)–C(1)	1.97 (1)
Ga(1)–S(1B)	2.323 (3)	Ga(1)–S(2A)	2.379 (5)
Ga(2)–S(1)	2.316 (4)	Ga(2)–S(2)	2.322 (3)
Ga(2)–C(2)	1.967 (1)	Ga(2)–S(1A)	2.392 (4)
S(1)–Ga(2A)	2.392 (4)	S(2)–Ga(1A)	2.379 (5)
S(2)–Ga(2B)	2.322 (3)		
S(1)–Ga(1)–C(1)	112.7 (2)	S(1)–Ga(1)–S(1B)	119.7 (2)
C(1)–Ga(1)–S(1B)	112.7 (2)	S(1)–Ga(1)–S(2A)	97.4 (1)
C(1)–Ga(1)–S(2A)	114.7 (5)	S(1B)–Ga(1)–S(2A)	97.4 (1)
S(1)–Ga(2)–S(2)	119.5 (1)	S(1)–Ga(2)–C(2)	112.8 (4)
S(2)–Ga(2)–C(2)	112.1 (4)	S(1)–Ga(2)–S(1A)	97.6 (1)
S(2)–Ga(2)–S(1A)	97.1 (1)	C(2)–Ga(2)–S(1A)	116.0 (4)
Ga(1)–S(1)–Ga(2)	117.3 (1)	Ga(1)–S(1)–Ga(2A)	82.5 (1)
Ga(2)–S(1)–Ga(2A)	82.4 (1)	Ga(2)–S(2)–Ga(1A)	82.9 (1)
Ga(2)–S(2)–Ga(2B)	117.7 (2)	Ga(1A)–S(2)–Ga(2B)	82.9 (1)

Surprisingly, the mass spectrum of an analytically pure sample of $[(^tBu)Ga(S)py]_3$ does not show any of the expected peaks, but only those due to the tetramer, $[(^tBu)GaS]_4$.[14] In fact, sublimation of $[(^tBu)Ga(S)py]_3$ at 230–250 °C under vacuum onto a cold finger also yields the tetramer is essentially quantitative yield (Scheme I). Thermogravimetric analysis data indicate that $[(^tBu)Ga(S)py]_3$ decomposes in the solid state at 120 °C. Heating a sample at this temperature results in a 32% mass loss (equivalent to loss of all pyridine, calculated 33.2%), leaving a white solid. On the basis of the ^1H NMR data, this material consists mainly of $[(^tBu)GaS]_8$ (ca. 60% yield), which is spectroscopically identical with that obtained from the thermolysis of $[(^tBu)GaS]_4$ in pentane (see Experimental Section). A small amount (ca. 30%) of $[(^tBu)GaS]_6$ (**3**) has also been identified to be present from the ^1H NMR and mass spectral data (m/z = 953). A greater yield of $[(^tBu)GaS]_6$ is formed (ca. 50%) when samples are heated nearer the sublimation temperature. Crystals of compound **3** may readily be separated from $[(^tBu)GaS]_4$ and $[(^tBu)GaS]_8$ by physical separation of the hexagonally shaped crystalline material from the remaining powder.

(11) Twist-boat conformations have been previously observed for six-membered group 13/15 compounds $[R_2MER'_2]_3$; see for example: (a) Atwood, J. L.; Stucky, G. D. *J. Am. Chem. Soc.* **1970**, *92*, 285. (b) McLaughlin, G. M.; Sim, G. A.; Smith, J. D. *J. Chem. Soc., Dalton Trans.* **1972**, 2197. (c) Wells, R. L.; Purdy, A. P.; McPhail, A. T.; Pitt, C. G. *J. Organomet. Chem.* **1988**, *354*, 287. (d) Interrante, L. V.; Sigel, G. A.; Garbauskas, M.; Hejna, C.; Slack, G. A. *Inorg. Chem.* **1989**, *28*, 252.

(12) Tuck, D. G. In *Comprehensive Organometallic Chemistry*; Wilkinson, G., Stone, F. G. A., Abel, E. W., Eds.; Pergamon Press: Oxford, U.K., 1982; Vol. 1, Chapter 7.

(13) Atwood, D. A.; Jones, R. A.; Cowley, A. H.; Bott, S. G.; Atwood, J. L. *Polyhedron* **1991**, *10*, 1897.

(14) It should be noted that while the parent ion for $[(^tBu)GaS]_4$ (m/z = 636) is the same as for $[^tBu_3Ga_3(S)_3(py)_2]$, i.e., $3M^+ - py$ (m/z = 636), they may be readily differentiated from their respective isotope patterns.

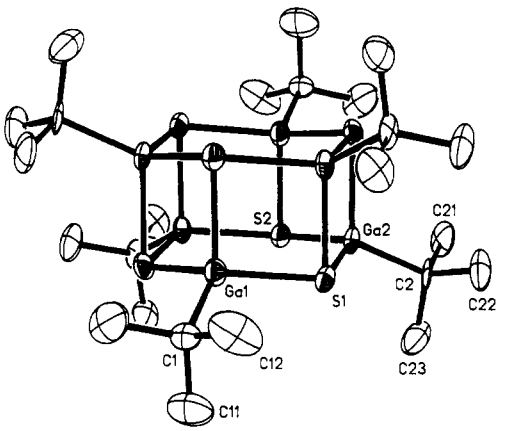

Figure 4. Molecular structure of $[(^tBu)GaS]_6$ (3). Thermal ellipsoids are shown at the 40% probability level, and hydrogen atoms are omitted for clarity.

The molecular structure of the hexamer has been determined by X-ray crystallography and is shown in Figure 4; selected bond lengths and angles are given in Table III. The Ga_6S_6 core can be described as a hexagonal prism with alternating Ga and S atoms. The chair conformation of each Ga_3S_3 face is unlike the planar structures observed for $[XAl(N^iPr)]_6$ (X = H, Me, Cl);[15] however, it is closely related to that observed for the anionic clusters $[Fe_6S_6X_6]^-$.[16] The Ga–S distances are of two types, those within (2.316 (3)–2.323 (3) Å) and those linking (2.379 (5)–2.392 (4) Å) the two Ga_3S_3 rings, both of which are significantly longer than those observed for the μ_2-sulfido bridges in 2 but are within the range observed for the μ_3-sulfido groups in $[(^tBu)GaS]_x$ (x = 4, 7) (see above).

The topological rearrangements observed for $[(^tBu)GaS]_x$ are, if not unique in cluster chemistry (other rearrangements being accompanied by changes in speciation), certainly the most extensive and reversible for a single well-characterized species. We propose that such cage transformations may be possible for a wider range of main-group clusters.

Gallium–Oxo Clusters. Our original synthesis of the gallium chalcogenide cubanes $[(^tBu)GaE]_4$ (E = S, Se, Te) involved the reaction of $Ga(^tBu)_3$ with the elemental chalcogen.[2,3] This reaction was proposed to proceed via the dichalcogenides (eq 1), which in the case of sulfur were

$$Ga(^tBu)_3 \xrightarrow{E\ (excess)} [(^tBu)_2Ga(\mu\text{-}EE^tBu)]_2 \xrightarrow{E\ (excess)} [(^tBu)GaE]_4 \quad (1)$$

isolated.[3] The oxygen analogue of the dichalcogenide $[(^tBu)_2Ga(\mu\text{-}OO^tBu)]_2$ is readily isolated as the sole product from the reaction of $Ga(^tBu)_3$ with O_2;[17] however, thermolysis of the peroxide results in an explosive decomposition, from which no gallium oxo species could be isolated. A modified route to the sulfido and seleno cubanes is the reaction of $Ga(^tBu)_3$ with H_2E via the unstable (but isolable in the case of sulfur) hydrochalcogenide complex (eq 2).[2,3]

$$Ga(^tBu)_3 + H_2E \xrightarrow{-^tBuH} [(^tBu)_2Ga(\mu\text{-}EH)]_2 \xrightarrow{\Delta} [(^tBu)GaE]_4 \quad (2)$$

(15) DelPiero, G.; Perego, G.; Cucinella, S.; Cesari, M.; Mazzei, A. *J. Organomet. Chem.* **1977**, *136*, 13.

(16) (a) Saak, W.; Henkel, G.; Pohl, S. *Angew. Chem., Int. Ed. Engl.* **1984**, *23*, 150. (b) Kanatzidis, M. G.; Hagen, W. R.; Dunham, W. R.; Lester, R. K.; Coucouvanis, D. *J. Am. Chem. Soc.* **1985**, *107*, 953. (c) Kanatzidis, M. G.; Salifoglou, A.; Coucouvanis, D. *Inorg. Chem.* **1986**, *25*, 2460. (d) Kanatzidis, M. G.; Salifoglou, A.; Coucouvanis, D. *J. Am. Chem. Soc.* **1985**, *107*, 3358.

(17) Power, M. B.; Cleaver, W. M.; Apblett, A. W.; Barron, A. R.; Ziller, J. W. *Polyhedron* **1992**, *11*, 477.

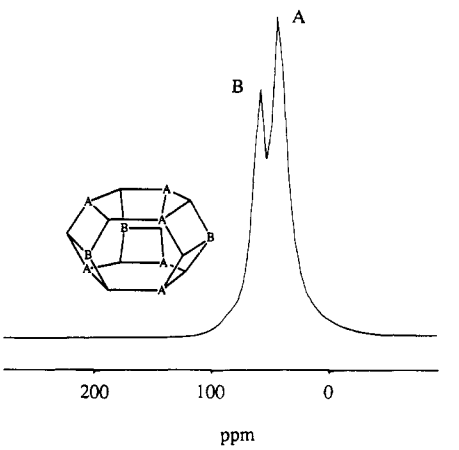

Figure 5. ^{17}O NMR spectrum of $[(^tBu)GaO]_9$ (4) showing the presence of two distinct oxo environments, i.e., those within (A) and those linking (B) the two parallel hexagonal faces (see inset).

We have previously reported that the hydrolysis of $Ga(^tBu)_3$ in noncoordinating solvents yields the trimeric hydroxide $[(^tBu)_2Ga(\mu\text{-}OH)]_3$.[17] Thermogravimetric analysis data indicate that $[(^tBu)_2Ga(\mu\text{-}OH)]_3$ decomposes exothermically in the solid state above 140 °C.[16] Heating a sample at this temperature results in a 29% mass loss (equivalent to ^tBuH) and the formation of a white powder, whose ^1H NMR spectrum consists of a very broad series of peaks consistent with a polymeric compound, possibly $[(^tBu)GaO]_x$. In contrast, heating $[(^tBu)_2Ga(\mu\text{-}OH)]_3$ in refluxing xylene for 48 h results in the formation of the first gallium–oxo cluster, $[(^tBu)GaO]_9$ (4), in high yield. We have unfortunately been unable to obtain crystals suitable for X-ray diffraction studies due to twinning problems; however, the medium-resolution CI mass spectrum shows peaks due to the parent ion (m/z = 1286), whose isotope pattern along with all subsequent peaks has been correctly confirmed by computer simulation. The ^1H and ^{13}C NMR spectra of 4 show the presence of two *tert*-butyl environments in a 1:2 ratio, while the ^{17}O NMR spectrum shows two oxide environments,[18] again in a 1:2 ratio (see Figure 5). To the best of our knowledge, the only nonameric, M_9X_9, cage compound of the main-group metals to be reported is $[Na(O^tBu)]_9$,[19] whose structure is derived from two parallel six-membered Na_3O_3 rings that are connected by three oxygen atoms and three sodium atoms, such that every oxygen is four-coordinate and each sodium has a coordination number of 3. Given the obvious structural analogy, i.e., replace O with Ga, and Na with O, we propose that compound 4 has the core structure shown in IV. All spectroscopic data are consistent with this proposal.

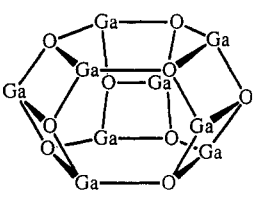

IV

Unlike the case for the sulfido clusters, we have not observed any controlled cage rearrangement for 4, although

(18) For a discussion of ^{17}O NMR chemical shifts in group 13 compounds, see: Apblett, A. W.; Warren, A. C.; Barron, A. R. *Chem. Mater.* **1992**, *4*, 167.

(19) Greiser, T.; Weiss, E. *Chem. Ber.* **1977**, *110*, 3388.

decomposition does occur upon thermolysis in the solid state to give a plethora of inseparable new species.

Structural Relationship of $[(^tBu)GaS]_x$ to Iron–Sulfur Clusters and Iminoalanes. The structures of the gallium–sulfido cages reported in this paper and in previous publications[2,3] are clearly part of a general class of main-group and transition-metal cluster compounds, i.e., $[LMX]_x$ and $[LMXR]_x$, where X is from group 15, 16, or 17;[20] however, it is of particular interest to compare them to two specific analogues, the iminoalanes and the iron–sulfur clusters.

The structures of $[(^tBu)GaS]_x$ (x = 4, 6, 7) find similarities with a number of iminoalanes[21-23] and related group 13–15 clusters.[24] While the overall geometries are indeed similar, i.e., cube, trigonal prism, etc., the structural features show trends as a consequence of the increased size of S^{2-} versus that of NR^{2-}.[25] These changes are most apparent in considering the distortions of the four- and six-membered faces of the clusters. While the former in the iminoalanes are almost exactly squares (N–Al–N = 88 (1)–91 (1)°, Al–N–Al = 88 (1)–91 (1)°), those for $[(^tBu)GaS]_4$ are distinctly rhombahedral (S–Ga–S = 97.3 (1)°, Ga–S–Ga = 82 (1)°). Similar distortions are observed for the six-membered faces; i.e., those in the iminoalanes are trigonally distorted (N–Al–N = 108 (1)–111 (1)°, Al–N–Al = 117 (1)–123 (1)°), while those in **1** and **3** are closer to hexagonal (S–Ga–S = 113.3 (1)–119.7 (2)°, Ga–S–Ga = 110.2 (2)–117.7 (2)°). Since Ga and Al are close in size,[25] these structural differences are consistent with increased nonbonding repulsive interactions across the faces, i.e., S···S versus N···N. It appears therefore that while the topologies of the gallium sulfido and iminoalane cages are comparable, the intimate structural features are determined predominantly by atom packing in a manner similar to that for ionic crystal lattices.[25]

In contrast to their topological relationships, the facile cage rearrangements observed for the gallium–sulfido clusters appear to be unique since they have not been reported for the iminoalanes. We note, however, that several iminoalanes are known in different forms, i.e., $[RAl(N^iPr)]_x$ (R = H, Me; x = 4, 6) and $[MeAl(NMe)]_x$ (x = 6, 7). It is probable therefore that, given the higher Al–N versus Ga–S bond strength, the activation barrier for cluster interconversion may be significantly higher for the iminoalanes than for the gallium–sulfido clusters and may only be observed outside experimental conditions presently investigated. In addition, no reports have been published of the reaction of iminoalanes with Lewis bases.

The study of iron–sulfur cage chemistry has been stimulated by the desire to understand the biochemical behavior of non-heme iron–sulfur proteins, specifically the four-iron ferrodoxins.[26] While the largest biologically relevant cluster is the cubane with a $[Fe_4S_4]^{2+/+}$ core,[27] other higher nuclearity clusters have been prepared.[28]

The hydrolytic and aqueous chemistry of the Ga^{3+} ion is similar to that of the ferric ion. In fact, properties have been inferred from one to the other; e.g., diamagnetic gallium analogues of siderophores have been useful in NMR studies,[29] since the ferric ion complexes are paramagnetic. The homology between Ga^{3+} and Fe^{3+} is based primarily upon their similarity in ionic radii for six-coordinate complexes (0.620 Å for Ga^{3+} compared to 0.645 Å for Fe^{3+}).[30] Given the analogies observed for gallium and iron aqueous chemistry,[31] it is perhaps not surprising that the gallium homologue of the Fe_4S_4 cubes prepared as synthetic representations for ferrodoxins is isolable. What is notable, however, is that $[(^tBu)GaS]_4$ (Ga–S = 2.359 (3) Å) is structurally similar not to the isoelectronic $[CpFeS]_4$ (Fe–S = 2.20 (8)–2.26 (4) Å)[32] but to the mixed-valence (formally $Fe^{III}Fe^{II}_3$) trianions $[(X)FeS]_4^{3-}$ (Fe–S = 2.297 (6)–2.351 (9) Å).[33]

As we have noted above, the iron analogues of **3** have been previously reported; however, in one case a cage rearrangement occurs upon heating (eq 3).[34] Although a

$$2[Fe_6S_6Cl_6]^{3-} \rightarrow 3[Fe_4S_4Cl_4]^{2-} \quad (3)$$

wide number of core conversions are known, i.e., those in which the iron–sulfur–ligand ratio is changed,[35] the reaction in eq 3 is the only one comparable to the facile topological rearrangements observed for $[(^tBu)GaS]_x$.

Finally, we note that while a cluster with a $[Fe_3S_3]$ cyclic core, in which the irons are tetrahedral and the sulfurs bifurcating, has been structurally characterized in a 7 Fe ferredoxin from *Azotobacter vinelandii*,[36] no synthetic analogues have been reported, making, we believe, compound **2** the sole representation of this class of core compound.

Experimental Section

Melting points were determined in sealed capillaries and are uncorrected. Thermogravimetric and differential thermal analysis data were measured on a Seiko 200 TG/DTA instrument. Mass spectra were recorded using a JEOL AX-505H mass spectrometer and associated data system. An electron beam energy of 70 eV was used for EI mass spectra. Isobutane was used as a reagent gas for CI mass spectra. All spectra were recorded at 1500 mass resolution. Reported m/z values are for the predominant ion within the isotope pattern for each signal. IR spectra (4000–400 cm^{-1}) were recorded on a Nicolet 5ZDX FTIR spectrometer as

(20) For a comprehensive review on cage compounds of main-group metals, see: Veith, M. *Chem. Rev.* **1990**, *90*, 3.
(21) Cucinella, S.; Salvatori, T.; Busetto, C.; Perego, G.; Mazzei, A. *J. Organomet. Chem.* **1974**, *78*, 185.
(22) Cesari, M.; Perego, G.; DelPiero, G.; Cucinella, S.; Cernia, E. *J. Organomet. Chem.* **1974**, *78*, 203.
(23) DelPiero, G.; Cesari, M.; Dozzi, G.; Mazzei, A. *J. Organomet. Chem.* **1977**, *129*, 281.
(24) Cowley, A. H.; Jones, R. A.; Mardones, M. A.; Atwood, J. L.; Bott, S. G. *Angew. Chem., Int. Ed. Engl.* **1990**, *29*, 1409.
(25) Pauling, L. *The Nature of the Chemical Bond*; Cornell University Press: Ithaca, NY, 1948.
(26) Lovenberg, W., Ed. *Iron-Sulfur Proteins*; Academic Press: New York, 1973; Vol. 1. *Ibid.*, 1974, Vol. 2. *Ibid* 1976, Vol. 3.
(27) Berg, J. M.; Holm, R. H. In *Metal Ions in Biology*; Spiro, T. G., Ed.; Interscience: New York, 1982; Vol. 4, Chapter, 1.
(28) See for example: (a) Christou, G.; Holm, R. H.; Sabat, M.; Ibers, J. A. *J. Am. Chem. Soc.* **1981**, *103*, 6269. (b) Hagen, K. S.; Watson, A. D.; Holm, R. H. *J. Am. Chem. Soc.* **1983**, *105*, 3905. (c) Strasdeit, H.; Krebs, B.; Henkel, G. *Inorg. Chem.* **1984**, *23*, 1816. (d) Strasdeit, H.; Krebs, B.; Henkel, G. Z. *Naturforsch., B* **1987**, *42*, 565. (e) Zenello, P. *Coord. Chem. Rev.* **1988**, *83*, 199. (f) Agresti, A.; Bacci, M.; Cecconi, F.; Ghilardi, C. A.; Midollini, S. *Inorg. Chem.* **1985**, *24*, 689. (g) Pohl, S.; Saak, W. *Angew. Chem., Int. Ed. Engl.* **1984**, *23*, 907.
(29) (a) Bergeron, R. J.; Kline, S. J. *J. Am. Chem. Soc.* **1983**, *106*, 3089. (b) Llinas, M.; Wilson, D. M.; Neilands, J. B. *Biochemistry* **1973**, *12*, 3836.
(30) Shannon, R. D. *Acta Crystallogr., Sect. A* **1976**, *32*, 751.
(31) See for example: (a) Plaha, D. S.; Rogers, H. J. *Biochem. Biophys. Acta* **1983**, *769*, 246. (b) Müller, G.; Raymond, K. N. *J. Bacteriol.* **1984**, *160*, 304. (c) Harris, W. R.; Weitl, F. L.; Raymond, K. N. *J. Am. Chem. Soc.* **1981**, *103*, 2667. (d) Borgias, B. A.; Barclay, S. J.; Raymond, K. N. *J. Coord. Chem.* **1986**, *15*, 109. (e) Martell, A. E.; Smith, R. M. *Critical Stability Constants*; Plenum Press: New York, 1982, and references therein.
(32) Toan, T.; Teo, B. K.; Ferguson, J. A.; Meyer, T. J.; Dahl, L. F. *J. Am. Chem. Soc.* **1977**, *99*, 408.
(33) (a) Mascharak, P. K.; Hagen, K. S.; Spence, J. T.; Holm, R. H. *Inorg. Chim. Acta* **1983**, *80*, 157. (b) Hagen, K. S.; Watson, A. D.; Holm, R. H. *Inorg. Chem.* **1984**, *23*, 2984.
(34) Kanatzidis, M. G.; Dunham, W. R.; Hagan, W. R.; Coucouvanis, D. *J. Chem. Soc., Chem. Commun.* **1984**, 356.
(35) Snyder, B. S.; Holm, R. H. *Inorg. Chem.* **1988**, *27*, 2339 and references therein.
(36) (a) Stout, C. D.; Ghosh, D.; Pattabhi, V.; Robbins, A. H. *J. Biol. Chem.* **1980**, *255*, 1797. (b) Ghosh, D.; Furey, W., Jr.; O'Donnell, S.; Stout, C. D. *J. Biol. Chem.* **1981**, *256*, 4185. (c) Howard, J. B.; Lorsbach, T. W.; Ghosh, D.; Melis, K.; Stout, C. D. *J. Biol. Chem.* **1983**, *258*, 508.

Table IV. Summary of X-ray Diffraction Data

compd	[(ᵗBu)GaS]₇ (1)	[(ᵗBu)Ga(S)py]₃ (2)	[(ᵗBu)GaS]₆ (3)
empirical formula	$C_{28}H_{63}Ga_7S_7$	$C_{27}H_{42}Ga_3N_3S_3$	$C_{24}H_{52}Ga_6S_6$
cryst size, mm	0.27 × 0.37 × 0.40	0.21 × 0.20 × 0.51	0.55 × 0.43 × 0.25
cryst syst	monoclinic	monoclinic	orthorhombic
space group	$P2_1/n$	$P2_1/c$	$Cmca$
a, Å	10.490 (1)	9.377 (5)	20.67 (1)
b, Å	21.697 (5)	15.832 (4)	9.116 (5)
c, Å	41.383 (7)	22.471 (7)	20.90 (1)
β, deg	95.34 (1)	98.42 (3)	
V, Å³	9378 (3)	3300 (2)	3940 (4)
Z	8	4	4
density (calcd), g/cm³	1.575	1.437	1.604
abs coeff, mm⁻¹	4.268	2.641	4.375
radiation	Mo Kα (λ = 0.71073 Å), graphite monochromator		
temp, K	168	193	298
2θ range, deg	4.0–45.0	4.0–40.0	4.0–40.0
index ranges	$0 \le h \le 11$, $0 \le k \le 23$, $-44 \le l \le 44$	$0 \le h \le 9$, $0 \le k \le 15$, $-21 \le l \le 21$	$0 \le h \le 19$, $0 \le k \le 8$, $-20 \le l \le 20$
no. of collected rflns	11436	3602	2154
no. of indep rflns	10796	3026	962
no. of obsd rflns	7898 ($\|F_o\| > 4.0\sigma(\|F_o\|)$)	2374 ($\|F_o\| > 4.0\sigma(\|F_o\|)$)	736 ($\|F_o\| > 4.0\sigma(\|F_o\|)$)
weighting scheme	$w^{-1} = \sigma(\|F_o\|) + 0.0007(\|F_o\|)^2$	$w^{-1} = \sigma(\|F_o\|) + 0.0007(\|F_o\|)^2$	$w^{-1} = \sigma(\|F_o\|) + 0.0024(\|F_o\|)^2$
final R indexes	R = 0.059, R_w = 0.071	R = 0.047, R_w = 0.059	R = 0.058, R_w = 0.072
largest diff peak, e/Å³	0.75	0.78	1.18

Table V. Atomic Coordinates (×10⁴) and Equivalent Isotropic Displacement Coefficients (Å² × 10⁴) for [(ᵗBu)GaS]₆ (1)

	x	y	z	U(eq)		x	y	z	U(eq)
				Molecule 1					
Ga(1)	1572 (2)	2830 (1)	1774 (1)	305 (5)	C(8)	2359 (15)	5248 (7)	1979 (3)	491 (60)
Ga(2)	2023 (1)	4182 (1)	1575 (1)	289 (5)	C(9)	2739 (13)	1992 (7)	878 (3)	366 (52)
Ga(3)	1841 (1)	2736 (1)	1038 (1)	284 (5)	C(10)	3811 (15)	2199 (8)	682 (4)	555 (66)
Ga(4)	−1085 (1)	3241 (1)	1466 (1)	290 (5)	C(11)	3224 (14)	1588 (7)	1160 (3)	442 (57)
Ga(5)	−836 (2)	4783 (1)	976 (1)	321 (5)	C(12)	1701 (15)	1660 (7)	656 (4)	535 (64)
Ga(6)	1552 (1)	4355 (1)	627 (1)	322 (5)	C(13)	−2591 (14)	2933 (7)	1670 (4)	422 (56)
Ga(7)	−999 (2)	3602 (1)	541 (1)	325 (5)	C(14)	−2130 (15)	2500 (8)	1954 (3)	479 (61)
S(1)	3060 (3)	3273 (2)	1444 (1)	294 (12)	C(15)	−3305 (15)	3482 (7)	1788 (4)	492 (61)
S(2)	204 (3)	2414 (2)	1343 (1)	298 (12)	C(16)	−3429 (14)	2583 (7)	1418 (4)	496 (61)
S(3)	379 (3)	3741 (2)	1840 (1)	305 (12)	C(17)	−1767 (16)	5484 (7)	1135 (4)	506 (64)
S(4)	−1821 (3)	3834 (2)	1025 (1)	326 (12)	C(18)	−1882 (24)	5393 (11)	1492 (4)	1137 (119)
S(5)	1343 (3)	4782 (2)	1133 (1)	344 (12)	C(19)	−3092 (18)	5517 (11)	954 (6)	1290 (122)
S(6)	1130 (4)	3306 (2)	592 (1)	358 (13)	C(20)	−1122 (21)	6065 (9)	1083 (6)	1210 (128)
S(7)	−531 (3)	4637 (2)	422 (1)	351 (13)	C(21)	3181 (14)	4566 (7)	450 (4)	423 (57)
C(1)	2179 (13)	2310 (7)	2146 (3)	347 (52)	C(22)	3277 (17)	5275 (8)	436 (5)	685 (76)
C(2)	3487 (19)	2056 (10)	2108 (4)	898 (97)	C(23)	3198 (16)	4300 (10)	109 (4)	714 (80)
C(3)	1286 (20)	1782 (9)	2176 (6)	1076 (107)	C(24)	4267 (15)	4305 (9)	669 (4)	665 (75)
C(4)	2205 (24)	2691 (10)	2448 (4)	1011 (106)	C(25)	−2074 (13)	3077 (6)	232 (3)	305 (48)
C(5)	3151 (14)	4695 (7)	1870 (3)	339 (51)	C(26)	−1501 (15)	3045 (8)	−83 (4)	611 (70)
C(6)	4273 (14)	4918 (7)	1707 (3)	433 (56)	C(27)	−2119 (19)	2430 (7)	395 (4)	693 (77)
C(7)	3632 (14)	4320 (7)	2170 (3)	430 (55)	C(28)	−3425 (14)	3330 (8)	194 (4)	525 (63)
				Molecule 2					
Ga(8)	6541 (2)	9699 (1)	1902 (1)	314 (5)	C(36)	9185 (16)	7585 (8)	1804 (4)	590 (69)
Ga(9)	6972 (1)	8349 (1)	1692 (1)	293 (5)	C(37)	2382 (12)	9616 (7)	1828 (3)	313 (49)
Ga(10)	3868 (1)	9306 (1)	1603 (1)	299 (5)	C(38)	1648 (14)	9068 (8)	1929 (4)	512 (63)
Ga(11)	6736 (1)	9814 (1)	1165 (1)	309 (5)	C(39)	2826 (15)	10005 (8)	2108 (4)	529 (64)
Ga(12)	6400 (2)	8211 (1)	739 (1)	372 (6)	C(40)	1547 (16)	10008 (8)	1576 (3)	505 (61)
Ga(13)	4086 (2)	7779 (1)	1110 (1)	359 (6)	C(41)	7642 (14)	10540 (7)	1020 (4)	417 (55)
Ga(14)	3835 (2)	8959 (1)	677 (1)	366 (6)	C(42)	8264 (15)	10900 (8)	1299 (4)	644 (72)
S(8)	5346 (3)	8793 (2)	1964 (1)	327 (12)	C(43)	8748 (15)	10302 (8)	820 (4)	559 (66)
S(9)	5148 (3)	10137 (2)	1483 (1)	309 (12)	C(44)	6738 (16)	10926 (8)	801 (4)	631 (69)
S(10)	7981 (3)	9258 (2)	1561 (1)	307 (12)	C(45)	7876 (15)	7951 (8)	518 (4)	500 (63)
S(11)	5965 (4)	9258 (2)	717 (1)	398 (14)	C(46)	7673 (24)	7296 (12)	381 (6)	1257 (133)
S(12)	6283 (4)	7768 (2)	1247 (1)	371 (13)	C(47)	9054 (16)	7959 (13)	749 (5)	1146 (122)
S(13)	3097 (4)	8723 (2)	1169 (1)	390 (13)	C(48)	8040 (16)	8374 (10)	231 (3)	708 (80)
S(14)	4292 (4)	7926 (2)	556 (1)	404 (14)	C(49)	3205 (16)	7068 (8)	1289 (4)	541 (68)
C(29)	7146 (16)	10220 (7)	2279 (3)	447 (59)	C(50)	3549 (30)	6493 (9)	1154 (7)	1769 (188)
C(30)	7277 (23)	9829 (10)	2588 (4)	997 (107)	C(51)	1797 (22)	7158 (12)	1199 (8)	1931 (203)
C(31)	6330 (21)	10749 (10)	2310 (6)	1349 (123)	C(52)	3387 (29)	7063 (12)	1637 (4)	1803 (178)
C(32)	8493 (21)	10438 (12)	2244 (5)	1139 (119)	C(53)	2629 (16)	9445 (9)	377 (4)	497 (64)
C(33)	8095 (14)	7818 (6)	1984 (3)	369 (53)	C(54)	3306 (26)	9684 (20)	139 (6)	2706 (322)
C(34)	7325 (17)	7272 (8)	2079 (4)	586 (67)	C(55)	1579 (26)	9090 (12)	242 (8)	2154 (209)
C(35)	8615 (15)	8192 (8)	2292 (3)	488 (60)	C(56)	2189 (36)	9949 (13)	549 (7)	2393 (256)

[a] Equivalent isotropic U defined as one-third of the trace of the orthogonalized U_{ij} tensor.

Nujol mulls on KBr plates. ^{1}H and ^{13}C NMR spectra (in C_6D_6 unless otherwise stated) were recorded on a Bruker AM-500 spectrometer, and chemical shifts are reported in parts per million relative to external $SiMe_4$ in $CDCl_3$. ^{17}O NMR spectra were recorded on a Bruker WM-300 spectrometer (δ in parts per million relative to external H_2O). [(ᵗBu)GaS]$_4$ and [(ᵗBu)$_2$Ga(μ-OH)]$_3$ were prepared according to published procedures.[2,3,16] All manipulations were carried out under an atmosphere of dry nitrogen. Solvents

were distilled and degassed before use.

[(ᵗBu)GaS]₇ (1). [(ᵗBu)GaS]₄ (1.0 g, 1.57 mmol) was refluxed in hexane (50 mL) for 3–4 days. The resulting solution was reduced to dryness under vacuum, leaving a white solid. ^{1}H NMR analysis indicated this to be a new species containing only small amounts (<15%) of [(ᵗBu)GaS]₄. [ᵗBuGaS]₇ was obtained pure by fractional crystallization, being more soluble in hexane than [(ᵗBu)GaS]₄: yield 0.79 g, 80%. Compound 1 may also be prepared in a similar yield by heating a sample of [(ᵗBu)GaS]₄, under nitrogen at 175 °C, in a sealed tube for 1 week. Mp: >260 °C. MS (EI): m/z 1054 (7M⁺ – ᵗBu, 100%). MS (CI; isobutane): m/z 1112 (7M⁺, 25%), 1054 (7M⁺ – ᵗBu, 15%). IR (Nujol): 1172 (s), 1009 (m), 941 (w), 807 (s), 722 (w), 660 (w), 529 (w), 510 (w). NMR (C_6D_6): ^{1}H, 1.27 [27 H, s, C(CH_3)$_3$], 1.23 [9 H, s, C (CH_3)$_3$], 1.19 [27 H, s, C(CH_3)$_3$]; ^{13}C, 30.07 [C(CH$_3$)$_3$], 30.01 [C(CH$_3$)$_3$], 29.93 [C(CH$_3$)$_3$], 29.21 [C(CH$_3$)$_3$], 27.74 [C(CH$_3$)$_3$], 27.48 [C(CH$_3$)$_3$].

[(ᵗBu)GaS]₈. [(ᵗBu)GaS]₄ (1.0 g, 1.57 mmol) was refluxed in pentane (50 mL) overnight. The mixture was then evaporated to dryness under vacuum. ^{1}H NMR spectroscopy indicated a mixture of [(ᵗBu)GaS]₄ (75%) and [(ᵗBu)GaS]₈ (25%). Washing the crude product with pyridine (2 × 40 mL) resulted in the isolation of a white powder determined by ^{1}H NMR spectroscopy to be pure octamer: isolated yield ca. 10%. MS (EI): m/z 1214 (8M⁺ – ᵗBu, 100%), 1158 (8M⁺ – ᵗBu – H_2C=CMe_2, 20%), 1102 (8M⁺ – ᵗBu$_2$ – 2H_2C=CMe_2, 18%). IR (Nujol): 1173 (s), 1010 (m), 942 (w), 806 (m), 724 (w), 530 (w). NMR (C_6D_6): ^{1}H, 1.54 [s, C(CH_3)$_3$]; ^{13}C, 30.00 [C(CH_3)$_3$], 26.00 [C(CH$_3$)$_3$].

[(ᵗBu)Ga(S)py]₃ (2). Excess pyridine (ca. 50 mL) was added to [(ᵗBu)GaS]₄ (1.0 g, 1.57 mmol). The resulting suspension became warm, and after it was stirred for ca. 1 h, a clear solution resulted. The pyridine solvent was reduced in volume under vacuum to ca. 10 mL and the solution set aside at –25 °C overnight to give colorless crystals, which were filtered and dried under vacuum. The filtrate was then reduced to dryness, yielding more crude product: combined yield 1.34 g, 90%. Compound 2 may also be prepared from [(ᵗBu)GaS]$_x$ (x = 6–8). The reaction is less facile, requiring either longer reaction times (ca. 1–2 days) or heating to ensure complete reaction. Mp: 90–100 °C dec. IR (Nujol): 1604 (m), 1574 (w), 1212 (m), 1171 (w), 1156 (w), 1068 (m), 1038 (m), 1007 (m), 939 (w), 810 (m), 756 (m), 700 (s), 635 (m), 524 (w), 429 (m). NMR (C_5D_5N): ^{1}H, 8.71 [6 H, m, NCH], 7.54 [3 H, m, p-CH], 7.18 [6 H, m, o-CH], 1.20 [27 H, s, C(CH_3)$_3$]; ^{13}C, 149.89 [t, o-C, py], 135.53 [t, p-C, py], 123.51 [t, m-C, py], 30.12 [s, C(CH_3)$_3$], 24.90 [s, C(CH$_3$)$_3$].

[(ᵗBu)GaS]₆ (3). Solid [(ᵗBu)GaS(py)]$_3$ (1.0 g, 1.40 mmol) was heated to ca. 200–220 °C under vacuum (10^{-3} Torr). A small quantity of [(ᵗBu)GaS]₄ began to sublime after 15 min at this temperature and condensed on cooler parts of the flask. After about 1 h the heating was stopped, and the contents were cooled to room temperature. ^{1}H NMR spectroscopy indicated that the nonsublimed material remaining consisted mainly of one new species with some [(ᵗBu)GaS]₄ (ca. 15%) and [(ᵗBu)GaS]₈ (ca. 30%) also present. Some crystalline material was separated by hand, the crystals which were hexagonal in shape, and whose ^{1}H NMR indicated them to be the new species: yield 0.2 g, 50%. Mp: 230 °C (sublimes). MS (EI): m/z 897 (6M⁺ – ᵗBu, 60%), 636 (4M⁺, 35%), 579 (4M⁺ – ᵗBu, 100%). MS (CI; NH_3) m/z 970 (6M⁺ + NH_3, 25%), 953 (6M⁺, 30%), 897 (6M⁺ – ᵗBu, 15%). IR (Nujol): 1171 (s), 1007 (m), 941 (w), 807 (m), 722 (w), 529 (w). NMR (C_6D_6): ^{1}H, 1.23 [s, C(CH_3)$_3$].

[ᵗBuGaO]₉ (4). [(ᵗBu)$_2$Ga(OH)]$_3$ (2.0 g, 3.31 mmol) was refluxed in xylene (ca. 30 mL) for 2 days. The clear solution was cooled, and the xylene was removed under vacuum to leave a white residue. This was recrystallized from the minimum amount of toluene (ca. 5 mL) to yield colorless crystals: yield 1.27 g, 90%. Mp: >260 °C dec. MS (EI): m/z 1230 (9M⁺ – ᵗBu, 50%), 1114 (9M⁺ – ᵗBu–O, 10%), 553 (4M⁺ – O, 50%), 505 (4M⁺ – ᵗBu, 100%). MS (CI; isobutane): m/z 1286 (9M⁺, 65%). IR (Nujol): 1262 (w), 1185 (w), 1013 (w), 941 (w), 816 (m), 727 (s), 624 (s), 562 (s), 524 (s), 490 (w), 465 (m), 405 (s). NMR (C_6D_6): ^{1}H, 1.32 [27 H, s, C(CH_3)$_3$], 1.31 [54 H, s, C(CH_3)$_3$]; ^{13}C, 30.29 [C(CH_3)$_3$], 30.08 [C(CH_3)$_3$], 26.46 [C(CH$_3$)$_3$], 25.34 [C(CH$_3$)$_3$]; ^{17}O (20.4% ^{17}O enriched), 62.91 (1 O, s), 47.68 (2 O, s).

X-ray Crystallographic Studies. A crystal data summary is given in Table IV; fractional atomic coordinates are listed in Tables V–VII. X-ray data for compound 1 were collected on a Siemens P3 diffractometer, which is equipped with a modified LT-2 low-temperature system. Determination of Laue symmetry, crystal class, unit cell parameters, and the crystal's orientation matrix were carried out by previously described methods.[37] Intensity data were collected at 168 K using an ω-scan technique with Mo Kα radiation under the conditions described in Table IV.

All 11 436 data were corrected for absorption and for Lorentz and polarization effects and placed on an approximately absolute scale. The systematic extinctions observed were $0k0$ for $k = 2n + 1$ and $h0l$ for $h + l = 2n + 1$; the diffraction symmetry was

Table VI. Atomic Coordinates (×10⁴) and Equivalent Isotropic Displacement Coefficients (Å² × 10³) for [(ᵗBu)Ga(S)Py]₃ (2)

	x	y	z	U(eq)[a]
Ga(1)	2204 (1)	3659 (1)	3652 (1)	24 (1)
Ga(2)	3737 (1)	1486 (1)	3875 (1)	24 (1)
Ga(3)	3035 (1)	2740 (1)	5140 (1)	25 (1)
S(1)	3722 (3)	2708 (2)	3361 (1)	30 (1)
S(2)	2973 (3)	1420 (2)	4768 (1)	29 (1)
S(3)	1803 (3)	3770 (2)	4611 (1)	30 (1)
C(1)	2417 (11)	4776 (6)	3256 (4)	33 (4)
C(2)	1248 (11)	5383 (6)	3391 (5)	45 (4)
C(3)	2291 (12)	4650 (7)	2564 (4)	44 (4)
C(4)	3880 (11)	5139 (7)	3495 (5)	48 (4)
N(1)	152 (8)	3310 (5)	3218 (3)	26 (3)
C(5)	–1009 (11)	3611 (6)	3421 (4)	31 (4)
C(6)	–2394 (12)	3504 (7)	3115 (5)	42 (5)
C(7)	–2537 (13)	3059 (7)	2589 (6)	48 (5)
C(8)	–1363 (13)	2749 (7)	2370 (5)	42 (4)
C(9)	–12 (12)	2883 (6)	2699 (4)	33 (4)
C(10)	3166 (10)	474 (6)	3361 (4)	29 (4)
C(11)	4137 (13)	396 (8)	2884 (6)	67 (6)
C(12)	3280 (14)	–335 (7)	3740 (5)	60 (5)
C(13)	1627 (11)	569 (8)	3071 (5)	64 (5)
N(2)	5989 (8)	1290 (5)	4104 (3)	29 (3)
C(14)	6905 (12)	1690 (8)	3797 (6)	53 (5)
C(15)	8345 (13)	1549 (8)	3893 (6)	69 (6)
C(16)	8917 (12)	974 (7)	4335 (5)	49 (5)
C(17)	7974 (11)	560 (7)	4628 (5)	44 (5)
C(18)	6508 (11)	718 (6)	4506 (5)	33 (4)
C(19)	2759 (11)	2747 (7)	6007 (4)	36 (4)
C(20)	4066 (11)	2447 (7)	6434 (5)	47 (4)
C(21)	2355 (15)	3628 (9)	6186 (5)	78 (6)
C(22)	1493 (13)	2160 (10)	6067 (5)	75 (6)
N(3)	5162 (8)	3083 (6)	5109 (3)	29 (3)
C(23)	6191 (11)	2531 (7)	5298 (5)	42 (5)
C(24)	7651 (13)	2701 (9)	5297 (6)	61 (6)
C(25)	8042 (13)	3446 (9)	5066 (6)	55 (5)
C(26)	6971 (13)	4026 (7)	4852 (5)	41 (5)
C(27)	5528 (11)	3815 (7)	4885 (4)	34 (4)

[a] Equivalent isotropic U defined as one-third of the trace of the orthogonalized U_{ij} tensor.

Table VII. Atomic Coordinates (×10⁴) and Equivalent Isotropic Displacement Coefficients (Å² × 10³) for [(ᵗBu)GaS]₆ (3)

	x	y	z	U(eq)[a]
Ga(1)	0	2154 (2)	4247 (1)	36 (1)
Ga(2)	961 (1)	470 (2)	5713 (1)	35 (1)
S(1)	972 (1)	1884 (4)	4792 (2)	38 (1)
S(2)	0	169 (5)	6272 (2)	36 (2)
C(1)	0	3856 (19)	3664 (9)	39 (7)
C(11)	0	5272 (25)	4074 (13)	87 (11)
C(12)	612 (8)	3846 (19)	3250 (9)	92 (8)
C(2)	1693 (5)	898 (14)	6284 (6)	41 (5)
C(21)	1730 (7)	–282 (16)	6793 (7)	66 (6)
C(22)	2332 (6)	902 (19)	5894 (7)	72 (7)
C(23)	1586 (7)	2382 (17)	6592 (9)	77 (7)

[a] Equivalent isotropic U defined as one-third of the trace of the orthogonalized U_{ij} tensor.

(37) Churchill, M. R.; Lashewycz, R. A.; Rotella, F. J. *Inorg. Chem.* **1977**, *16*, 265.

$2/m$. The centrosymmetric monoclinic space group $P2_1/n$, a nonstandard setting of $P2_1/c$ (C^5_{2h}; No. 14), is uniquely defined.

All crystallographic calculations were carried out by using either the UCI-modified version of the UCLA Crystallographic Computing Package[38] or the SHELXTL PLUS program set.[39] The analytical scattering factors for neutral atoms were used throughout the analysis;[40a] the real ($\Delta f'$) and imaginary ($i\Delta f''$) components of anomalous dispersion[24b] were included. The quantity minimized during least-squares analysis was $\sum w(|F_o| - |F_c|)^2$, where $w^{-1} = \sigma(|F_o|) + 0.0007\,(|F_o|)^2$.

The structures were solved by direct methods (SHELXTL PLUS)[39] and refined by full-matrix least-squares techniques. Hydrogen atoms were included using a riding model with d(C–H) = 0.96 Å and U(iso) = 0.08 Å^2. There are two independent molecules in the asymmetric unit. Refinement of positional and thermal parameters led to convergence (see Table IV).

Crystals of compounds **2** and **3** were mounted directly onto the goniometer with silicon grease. Unit-cell parameters and intensity data were obtained by following previously detailed procedures,[41] using a Nicolet R3m/v diffractometer operating in the ω-scan mode. Data collection was controlled by using the Nicolet P3 program.[42] Empirical absorption corrections were applied to the data using the program PSICOR.[42] Crystal symmetry and space groups were determined by the program XPREP.[39] Further experimental data are given in Table IV.

The structures were solved using the direct-methods program XS,[39] which revealed the positions of most of the heavy atoms. Most but not all of the hydrogens were visible in the final difference map. Hydrogens were included as fixed-atom contributors in the final cycles; d(C–H) = 0.96 Å and U(iso) = 0.08 Å^2. Details of the refinement are given in Table IV. Atomic scattering factors and anomalous scattering parameters were as given in ref 40.

Acknowledgment. Financial support of this work was provided by the donors of the Petroleum Research Fund, administered by the American Chemical Society. Funds for the purchase of the Nicolet R3m/V diffractometer system were made available from the NSF under Grant CHE-85-14495. The Harvard MS Facility is supported by grants from the NSF and NIH. Dr. A. N. Tyler is gratefully acknowledged for assistance with the mass spectroscopic measurements.

Supplementary Material Available: Tables of bond lengths and angles, anisotropic thermal parameters, and hydrogen atom parameters for 1–3 (20 pages). Ordering information is given on any current masthead page.

OM9201674

(38) UCLA Crystallographic Computing Package; University of California: Los Angeles, 1981. Strouse, C. Personal communication.
(39) *SHELXTL-PLUS Users Manual*; Nicolet Instrument Corp.: Madison, WI, 1988.
(40) (a) *International Tables for X-ray Crystallography*; Kynoch Press: Birmingham, England, 1974; pp 99–101. (b) *Ibid.*, pp 149–150.
(41) Healy, M. D.; Wierda, D. A.; Barron, A. R. *Organometallics* **1988**, *7*, 2543.
(42) *P3/R3 Data Collection Manual*; Nicolet Instrument Corp.: Madison, WI, 1988.

C–H Activation of Ethene by Non-Cyclopentadienyl-Containing Iridium Complexes. Supporting Role of $iPr_2PCH_2CH_2OMe$ as Phosphine Ligand[1]

Michael Schulz and Helmut Werner*

Institut für Anorganische Chemie der Universität Würzburg, Am Hubland, D-8700 Würzburg, Germany

Received January 6, 1992

UV irradiation of *trans*-[IrCl(C_2H_4)($PiPr_3$)$_2$] (**4**) in toluene gives only small amounts of the hydrido(vinyl)iridium isomer [IrH(CH=CH_2)Cl($PiPr_3$)$_2$] (**5**). If, however, the photolysis is carried out in the presence of pyridine, a mixture of two isomers of [IrH(CH=CH_2)Cl(py)($PiPr_3$)$_2$] (**6a,b**) is formed in 88% yield. Displacement of pyridine by CO gives [IrH(CH=CH_2)Cl(CO)($PiPr_3$)$_2$] (**7**). Photolysis of *trans*-[IrCl(C_2H_4)(η^1-$iPr_2PCH_2CH_2OMe$)$_2$] (**8**) in toluene proceeds rapidly and leads to the quantitative formation of [IrH(CH=CH_2)Cl(η^1-$iPr_2PCH_2CH_2OMe$)(η^2-$iPr_2PCH_2CH_2OMe$)] (**9**). Compound **9**, which in solution shows a fluxional behavior ($\Delta G^{\ddagger}$ ca. 41 kJ/mol in toluene), also reacts with CO to give [IrH(CH=CH_2)Cl(CO)(η^1-$iPr_2PCH_2CH_2OMe$)$_2$] (**10**). The thermal reaction of **9** regenerates the π-ethylene complex **8**, whereas the carbonyl(hydrido)vinyl derivative **10** reacts in refluxing benzene to form ethylene and the four-coordinate carbonyliridium compound *trans*-[IrCl(CO)(η^1-$iPr_2PCH_2CH_2OMe$)$_2$] (**11**). The X-ray crystal structure of **7** has been determined (triclinic space group $P\bar{1}$ (No. 2) with a = 8.848 (3) Å, b = 9.876 (4) Å, c = 16.200 (6) Å, α = 72.38 (2)°, β = 75.10 (2)°, γ = 78.62 (2)°, and Z = 2).

Introduction

Ethylene is certainly one of the most prominent ligands in π-complex chemistry.[2] If a transition-metal compound [ML_n] reacts with C_2H_4, it was until recently the general belief that an interaction between M and C_2H_4 can only occur via the C=C double bond. However, in 1985 it was shown by Stoutland and Bergman that the reaction of ethylene with a coordinatively unsaturated metal center such as iridium in [(C_5Me_5)(PMe_3)Ir] leads not only to coordination but also to oxidative addition to give a hy-

Scheme I

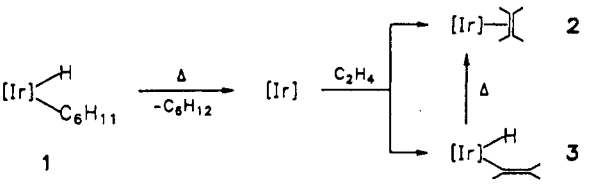

[Ir] = (C_5Me_5)(PMe_3)Ir

(1) Studies on C–H Activation. 7. Part 6: Werner, H.; Roder, K. *J. Organomet. Chem.* **1989**, *367*, 339–342.
(2) (a) Elschenbroich, C.; Salzer, A. *Organometallchemie*; Teubner Studienbücher: Stuttgart, Germany, 1988. (b) Collman, J. P.; Hegedus, L. S.; Norton, J. R.; Finke, R. G. *Principles and Application of Organotransition Metal Chemistry*; University Science Books: Mill Valley, CA, 1987. (c) Yamamoto, A. *Organotransition Metal Chemistry*; Wiley: New York, 1986. (d) Crabtree, R. H. *The Organometallic Chemistry of the Transition Metals*; Wiley: New York, 1988.

0276-7333/92/2311-2790$03.00/0